Published by IOP Publishing for Sissa Medialab

Received: *August 3, 2019*
Revised: *August 21, 2019*
Accepted: *February 27, 2020*
Published: *March 20, 2020*

Feasibility study of using polyacrylamide gel dosimeter as brain equivalent material in therapeutic energy range of X-rays

L. Teimoori Khandan,[a] S. Kashian[b] and P. Rezaeian[b,1]

[a] *Department of Physics, Faculty of Science, Islamic Azad University Hamedan Branch, Mousivand Blvd, PO Box 6518115743, Hamedan, Iran*

[b] *Radiation Application Research School, Nuclear Science and Technology Research Institute (NSTRI), AEOI, North Kargar Street, PO Box 1439951113, Tehran, Iran*

E-mail: prezaeian@aeoi.org.ir

Abstract: In this paper the feasibility study of using polyacrylamide gels as a brain equivalent material has been performed. Thus, the parameters of mass energy absorption coefficient ($\frac{\mu_{en}}{\rho}$), mass stopping power ($\frac{S}{\rho}$), effective atomic number (Z_{eff}), mass attenuation coefficient ($\frac{\mu_{eff}}{\rho}$) and absorbed dose delivered to polyacrylamide gel (D) were determined for this gel using analytical and Monte Carlo methods and were compared with brain reference material. The calculation results reveal that the relative difference between the calculated $\frac{\mu_{en}}{\rho}$, $\frac{S}{\rho}$, Z_{eff}, $\frac{\mu_{eff}}{\rho}$ and D for polyacrylamide gel and those for brain are 1.32%, less than 1%, less than 2%, less than 4% and less than 1%, respectively in therapeutic energy range. Consequently, like water, polyacrylamide gel can be also used for designing and construction of head and neck phantoms applied for validation of medical algorithms used in treatment planning systems. The advantage of using polyacrylamide gel as a brain equivalent material in comparison to water is that this gel is a reliable X and gamma rays dosimeter applicable for three dimensional dose distribution determination. Also, other advantages of this gel are its low price, availability and forming it in different sizes and shapes. These properties of the polyacrylamide gel make it beneficial as brain equivalent material in designing and construction of head and neck phantoms.

Keywords: Algorithms and Software for radiotherapy; Dosimetry concepts and apparatus; Instrumentation for gamma-electron therapy

[1] Corresponding author.

https://doi.org/10.1088/1748-0221/15/03/P03016

2020 JINST 15 P03016

Contents

2020 JINST 15 P03016

1 Introduction

Irradiation of head and neck using X-rays is known as one of the essential methods to treat the cancers of this part of body. Any failure in this treatment method can lead to destruction or deterioration of brain cells. So, in a radiotherapy procedure the effects of the radiation on the tumor or cancer cells have to be enhanced while the damages of the healthy tissues have to be minimized.

In a radiotherapy procedure, before the irradiation, a three dimensional dose distribution is required to calculate the absorbed dose delivered to tumor or cancer cells and the one received by the health tissues. Treatment planning systems (TPS) calculate this three dimensional dose distribution using different correction or model based algorithms [1–4]. Because of the essential role of algorithms used by TPS, the validation of them has to be performed for different organs and tissues using simulation or experimental methods [5–9].

The validation of the medical algorithms used by TPS in head and neck is one of the most important issues in the clinical radiotherapy due to the presence of surface curvature, air cavities, bony structure, inhomogeneous structure as well as vital organs such as brain in these regions of human body [10–13]. Consequently, many investigations have been performed to validate different algorithms in head and neck by constructing inhomogeneous head and neck phantoms [10, 12]. Different materials such as glass, human bone, plastic, polystyrene, Perspex, acrylonitrile butadiene

styrene, polycarbonate, polyurethane etc. have been used in construction of these phantoms [12–17]. Because the water can be considered to be a suitable substitute for brain [18], in head phantoms manufactured by different researchers, water is applied as the brain. Although water is usually utilized as a substitute for brain, it cannot be used as a dosimeter. So, in experimental measurements in order to evaluate of the medical algorithms, the absorbed dose delivered to water has to be determined using other dosimetry techniques such as ionization chamber, thermoluminescence dosimeters, radiographic films etc.. The material of these dosimeters differs with water, so this difference can influence dosimeter response and its accuracy [19]. Moreover, as mentioned above, the medical algorithms employed in TPS calculated a three dimensional absorbed dose in the irradiation of target region. Thus, in order to confirm the validation of these algorithms, the dose distribution in three dimensional should be measured, accurately. The above dosimetry methods can determine one or two dimensional dose distribution.

To overcome the challenges of the effect of surrounding medium on dosimeter response and determination of three dimensional absorbed dose, a brain equivalent material applicable for three dimensional dosimetry have to be used for the construction of head and neck phantom. To this purpose, for different material, dosimetry properties and parameters such as mass energy absorption coefficient, mass attenuation coefficient, mass stopping power, effective atomic number and absorbed dose delivered have to be investigated. One of the materials with reliable dosimetry properties used for determination of three dimensional dose distribution is polyacrylamide gel. This gel has been used as a gamma irradiation dosimeter since 1961 [20, 21]. In recent years, in order to improve the dosimetry properties of polyacrylamide gel different impurities such as inorganic salts, magnesium chloride, gold nanoparticle etc. were added to it [22–24].

The dosimetry properties of polyacrylamide gel, its price, availability, simple synthesis method and fabrication in any shape and size may make it a suitable candidate for fabrication of phantoms.

Also, these dosimeters can easily be readout using magnetic resonance imaging (MRI), optical and X-ray computed tomography (CT), Raman spectroscopy, and ultrasound [25–29].

To use this gel as brain, it has to be evaluated in term of mass energy absorption coefficient, mass attenuation coefficient, mass stopping power effective atomic number and absorbed dose delivered to it.

So, the purpose of this work is to evaluate polyacrylamide gel as brain tissue equivalent material. So, this material and some other materials such as water, PMMA, polyethylene, paraffin and nylon were examined with respect to mass energy absorption coefficient (μ_{en}/ρ), mass attenuation coefficient (μ/ρ), mass stopping power (S/ρ) and effective atomic number (Z_{eff}) in the therapeutic energy ranges. The calculated values are compared with brain reference material given in ICRU report 44 [30]. Further, the absorbed dose delivered to polyacrylamide gel and water were calculated in 6MV and 18 MV radiation fields of Siemens Primus medical accelerator using Monte Carlo simulations and were compared with absorbed dose delivered to brain reference material.

2 Materials and methods

To evaluate the polyacrylamide gel as a brain tissue-equivalent material in the therapeutic energy interval μ_{en}/ρ, μ/ρ, S/ρ and Z_{eff} of this gel and other material have to be determined and compared with reference to brain tissue. For calculating of these parameters knowing the elemental compo-

2020 JINST 15 P03016

Table 1. The atomic composition (%) and mass density of investigated.

Material	Brain (ICRU-44)	polyacrylamide	PMMA	Water	Nylon 6/10	Paraffin	Polyethylene
Density (g/cm^2)	1.03	1.02	1.19	1.00	1.14	0.93	0.93
H	1.00×10^{-1}	1.00×10^{-1}	8.00×10^{-2}	1.10×10^{-1}	1.10×10^{-1}	1.50×10^{-1}	1.40×10^{-1}
C	8.00×10^{-2}	8.00×10^{-2}	6.00×10^{-1}	–	6.80×10^{-1}	8.50×10^{-1}	8.60×10^{-1}
N	3.00×10^{-2}	3.00×10^{-2}	–	–	1.00×10^{-1}	–	–
O	7.90×10^{-1}	7.90×10^{-1}	3.20×10^{-1}	8.90×10^{-1}	1.10×10^{-1}	–	–
Na	1.80×10^{-3}	–	–	–	–	–	–
Mg	2.00×10^{-4}	–	–	–	–	–	–
P	3.50×10^{-3}	–	–	–	–	–	–
S	1.80×10^{-3}	–	–	–	–	–	–
Cl	2.40×10^{-3}	–	–	–	–	–	–
K	3.10×10^{-3}	–	–	–	–	–	–

sition of the material is necessary. The mass fractions of each element in investigated materials as well as their mass densities are tabulated in table 1. It should be mentioned that the polyacrylamide gel with concentration of 15% (W/V) was considered.

2.1 Analytical calculations

2.1.1 Calculation of mass energy absorption coefficient

To calculate the values of the mass energy absorption coefficient for polyacrylamide gel and other materials given in table 1, this coefficient was taken from reference [31] for each element of considered materials Using the mixture rule written in eq. (2.1), the mass energy absorption coefficient was calculated for polyacrylamide gel and other materials.

$$\left(\frac{\mu_{\text{en}}}{\rho}\right)_{\text{Mat}} = \sum_i w_i \left(\frac{\mu_{\text{en}}}{\rho}\right)_i \tag{2.1}$$

Where $\left(\frac{\mu_{\text{en}}}{\rho}\right) i$, is the mass energy absorption coefficient of ith element in material and w_{i} is the weight fraction of ith element.

2.1.2 Calculation of mass stopping power of electrons

To specify the mass stopping power for electrons, the value of mass stopping power for electrons in different materials was extracted from the NIST library [32]. Using these values, the mass stopping power of materials for electron can be calculated as

$$\left(\frac{S}{\rho}\right)_{\text{Mat}} = \sum_i w_i \left(\frac{S}{\rho}\right)_i \tag{2.2}$$

In this equation $\left(\frac{S}{\rho}\right) i$ is the mass stopping power of ith element for electrons.

2.2 Calculation of effective atomic number

The effective atomic number of different material was specified employing the Auto-Z_{eff} code [33]. This code can compute the effective atomic number as a function of energy as well as average and spectral-weighted means. This code was developed using the Microsoft Visual Basic.NET in 2012 by Taylor et al.. To determine the effective atomic number of polyacrylamide gel and different materials using this code, elements and the corresponding fractional components were imported to code according to table 1.

2.3 Monte Carlo simulations

2.3.1 Calculation of the mass attenuation coefficient

The mass attenuation coefficients were calculated by using Beer-Labmert law expressed as:

$$I = I_0 e^{-\mu x} \tag{2.3}$$

Where I_0 and I are the number of photons before and after attenuation, respectively. So, x is also the thickness of the considered slab. To calculate the linear attenuation coefficient for different energies in the therapeutic energy interval using eq. (2.3), Monte Carlo simulations were performed.

Monte Carlo simulations were done using MCNP.4C code [34]. Using the experimental setup similar to the setup used in reference [18] a geometrical configuration was implemented. In various energies, the different materials depicted in table 1 with different thickness were placed in the geometrical configuration shown in figure 1.

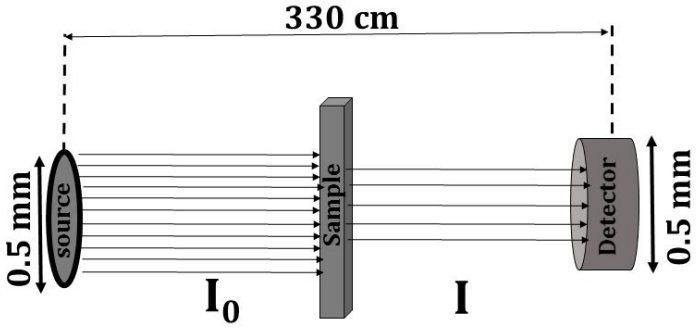

Figure 1. Schematic diagram of geometrical configuration used to determine the mass attenuation coefficient.

In each thickness, the values of I_0 and I were determined utilizing F2 tally. For a given material in a known energy the values of $-\ln\left(\frac{I}{I_0}\right)$ as a function of x were plotted, and the slop of the line fitted to plot data was taken into account as linear mass attenuation coefficient. Using the density of each material the mass attenuation coefficient was calculated.

2.3.2 Calculation of the absorbed dose delivered to the brain

The Absorbed dose delivered to polyacrylamide gel and water was calculated using MCNP.4C code. To simulated the head, a computational Snyder head phantom [35] with its curved surfaces, heterogeneous compositions and appropriate biological materials was modelled in the code. This phantom consists of three ellipsoids corresponding to skin, cranium and brain as shown in figure 2.

2020 JINST 15 P03016

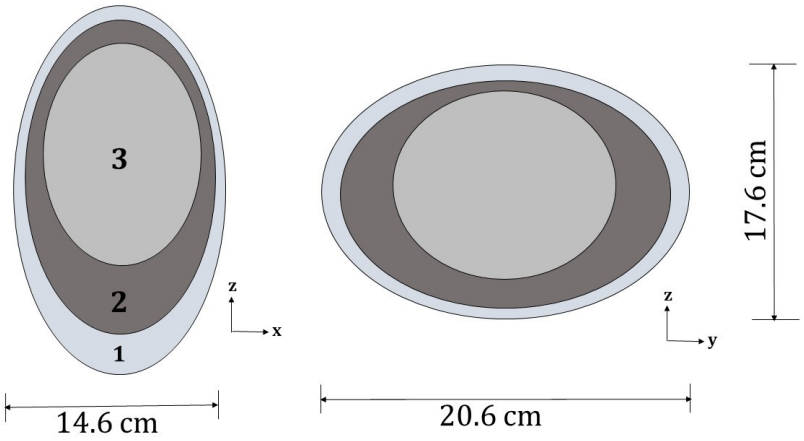

Figure 2. Schematic cross view of Snyder head phantom in $y = 0$ and $x = 0$ plane. The region (1), (2) and (3) are skin, cranium and brain, respectively.

Also the mathematical model of the Snyder head phantom is expressed as:

$$\left(\frac{x}{6}\right)^2 + \left(\frac{y}{9}\right)^2 + \left(\frac{z-1}{6.5}\right)^2 = 1 \tag{2.4}$$

$$\left(\frac{x}{6.8}\right)^2 + \left(\frac{y}{9.8}\right)^2 + \left(\frac{z}{8.3}\right)^2 = 1 \tag{2.5}$$

$$\left(\frac{x}{7.3}\right)^2 + \left(\frac{y}{10.3}\right)^2 + \left(\frac{z}{8.8}\right)^2 = 1 \tag{2.6}$$

The equations (2.4), (2.5) and (2.6) represent brain-cranium boundary, cranium-skin boundary and skin-air boundary, respectively.

The simulations were performed in radiation fields of 6MV and 18 MV Siemens Primus medical X-ray accelerators with X-ray spectrum similar to what is used in reference [36]. Also, the field size and source to surface distance were 10×10 cm^2 and 100 cm, respectively. For each radiation field the region which presents the brain (region 3 in figure 2) was filled with polyacrylamide gel, water and brain-ICRU44 [30]. The absorbed dose delivered to each material was calculated in dosimetry cell in the center of brain region using F4 tally. It should be mentioned that in MCNP simulation no energy cutoff was considered.

3 Result and discussion

3.1 The mass energy absorption coefficient

The value mass energy absorption coefficient of polyacrylamide gel and the other materials were calculated using eq. (2.1). Also, the mass energy absorption coefficient of the brain reference material was extracted from NIST data library [31].The ratio of mass energy absorption coefficient of polyacrylamide gel to brain is shown in figure 3. This ratio is also specified for other materials.

According to this figure, in the energy range of 1 to 3 MeV the mass absorption coefficient of nylon and the brain are the same approximately. Further, in the rest of the energy range, the values of the mass absorption coefficient of water and polyacrylamide are close to the mass absorption

2020 JINST 15 P03016

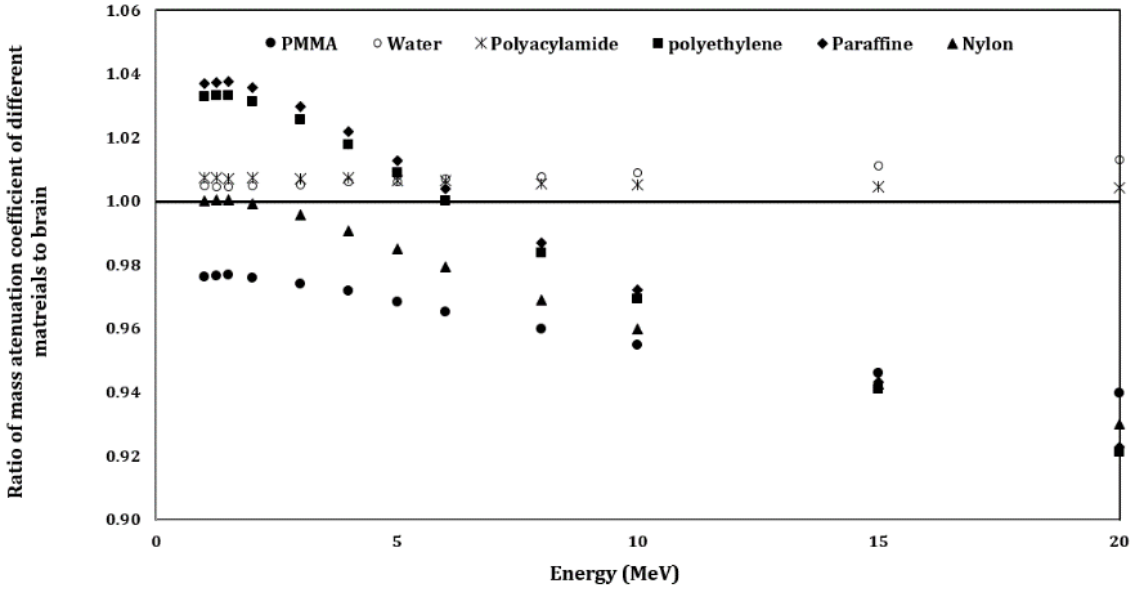

Figure 3. The ratio of mass energy absorption coefficient of different materials to the brain. The solid line shows the ratio of one.

coefficient of the brain. In other words, there is a relative difference less than 1.32% between the mass absorption energy coefficients of the polyacrylamide gel and the brain.

3.2 The mass stopping power of electrons

Using eq. (2.2) the mass stopping power of electrons in material investigated in this paper was calculated and the ratio of the mass stopping power of materials to the brain in the interested energy range was specified. This ratio is depicted in figure 4.

Figure 4 shows that the values of the stopping powers ratio are in the interval of 0.97 and 1.05. The variation of the stopping power ratio as a function of energy is smooth. The relative difference between the mass stopping power of polyacrylamide gel and brain is less than 1%.

3.3 The effective atomic number

Using Auto Zeff code, the effective atomic number of different materials was calculated. The obtained values are depicted in figure 5. In this figure, the effective atomic number of the brain is also shown with a solid line.

As shown in this figure, the values of the effective atomic number of the brain are between 3.31 and 3.90 in the energy interval of 1 to 20 MeV. The relative difference of the effective atomic number of water and polyacrylamide with the brain is less than 2% and 3%, respectively. It means that the atomic composition of water and polyacrylamide is similar to the brain.

3.4 The mass attenuation coefficient

Using MCNP.4C code, for each material, in a known energy, the number of the incident photons before attenuation (I_0) and after attenuation (I) were determined with statistical uncertainty less than 0.01% with the number of histories about 3×10^6 particles using F2 tally for different thicknesses.

2020 JINST 15 P03016

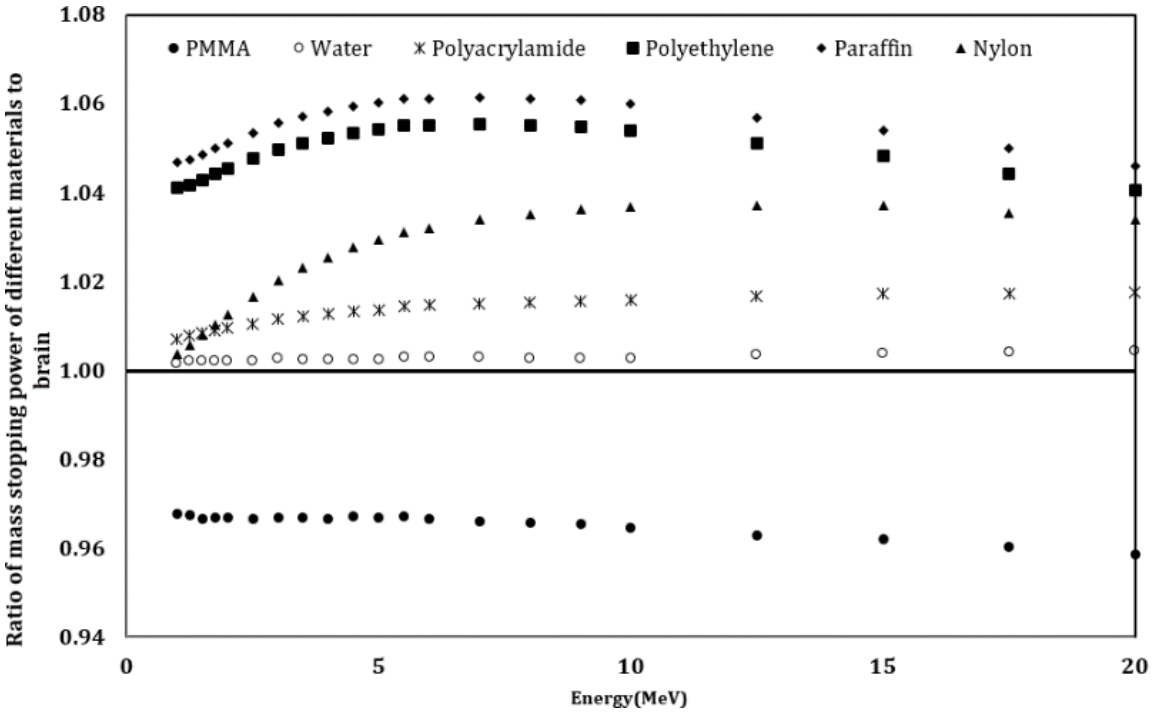

Figure 4. The ratio of mass stopping power of different materials to the brain. The ratio of one is depicted by a solid line.

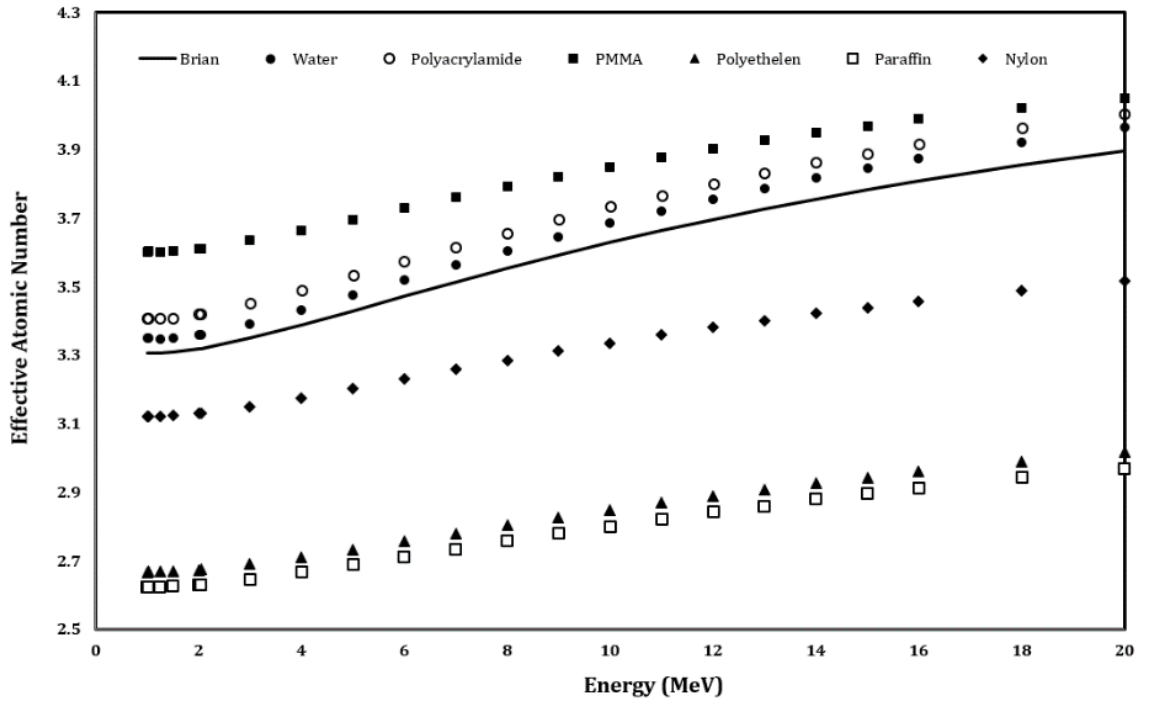

Figure 5. Values of effective atomic number as function of energy calculated using Auto Z_{eff} code.

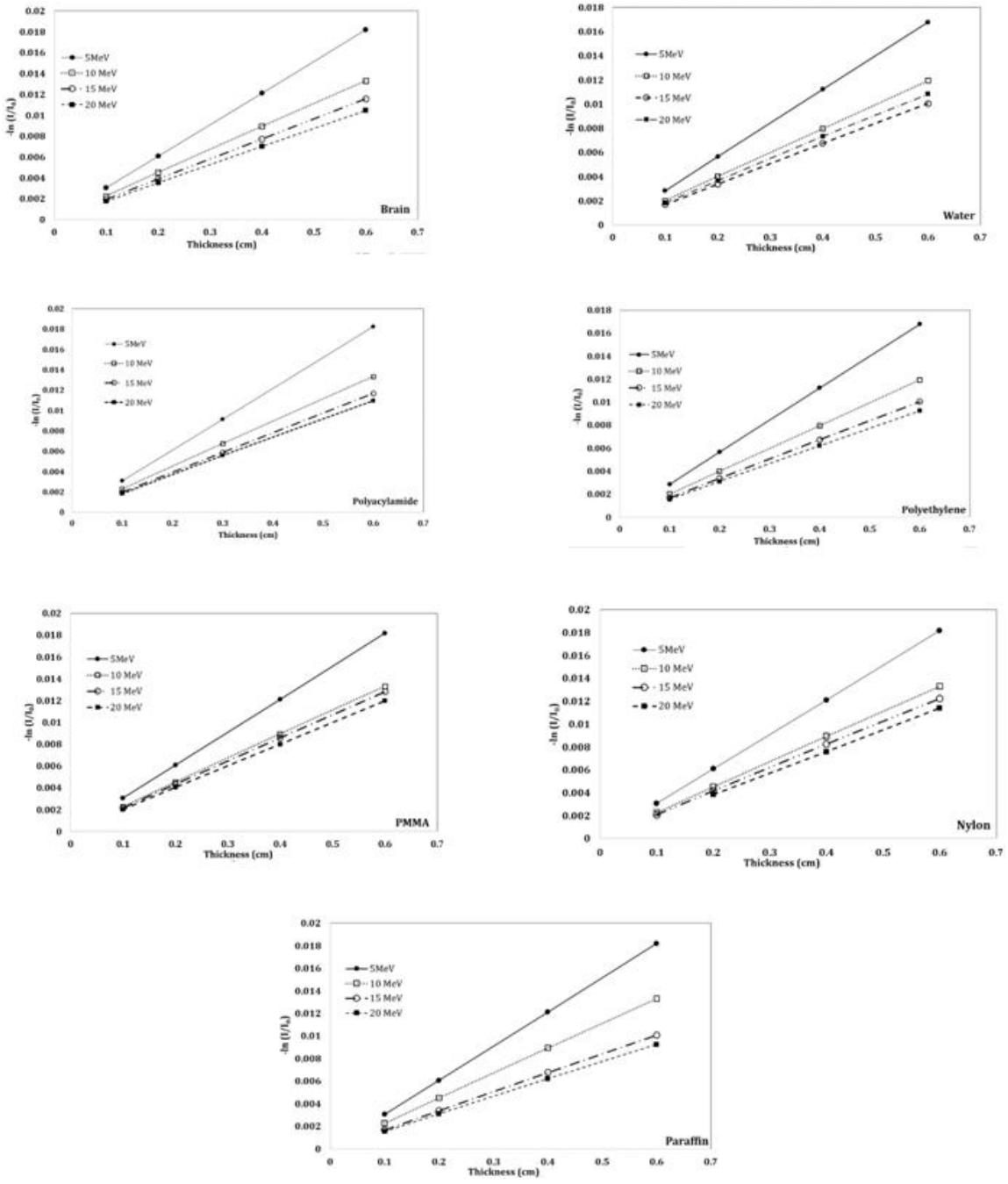

Figure 6. Variation of $\ln(I/I_0)$ as function of thickness used to calculate effective attenuation coefficient in different materials.

In figure 6, for the brain, water, polyacrylamide, PMMA, polyethylene, paraffin and nylon the variations of $-\ln(I/I_0)$ as a function of the thickness in different energy are depicted.

For each material in a known energy showing in figure 6, the value of the linear effective attenuation coefficient is determined. In order to calculate the uncertainty of the mass attenuation coefficnt, the effective vaiance method was used to fitt the data [37]. Using this method the

2020 JINST 15 P03016

uncertainty of mass attenuation coefficent was estimated (less than 1%) by taking into account the statistical uncertaintiy of I and I_0. The ratio of the mass effective attenuation coefficient of interested materials to brain was calculated as given in table 2.

Table 2. The ratio of the mass attenuation coefficient (cm^2/g) of the interested materials to the brain.

Energy (MeV)	Water	Polyacrylamide Gel	Paraffin	Polyethylene	Nylon	PMMA
5	0.99	1.00	0.98	0.92	1.11	0.97
10	1.00	1.00	0.90	0.90	1.08	1.00
15	0.99	1.01	0.87	0.87	1.06	1.00
20	0.94	0.96	0.81	0.81	0.99	0.94

As shown in this table, the relative difference between the mass attenuation coefficient between brain and polyacrylamide gel is less than 4%.

3.5 Calculation of delivered absorbed dose

According to the results of the previous sections, it can be concluded that polyacrylamide gel and water are closer to brain reference material by considering the mass energy absorption coefficient, mass stopping power, effective atomic number as well as mass attenuation coefficient. So, for Monte Carlo simulations the region of the brain in the computational head phantom (region 3 in figure 2) was filled with polyacrylamide gel and water. The absorbed dose in the dosimetry cell in the center of brain was calculated with statistical uncertainty less than 1% the number of histories about 3×10^6 particles and was compared with absorbed dose delivered to the brain reference material. The results of this comparison are shown in table 3.

Table 3. The values of absorbed dose in different materials in the 6 and 18 MV radiation fields of Siemens Primus medical X-ray accelerator.

	Absorbed Dose (mGy/emitted photon)	
Material	**6MV**	**18MV**
Brain	0.208±0.002	0.387±0.003
Polyacrylamide	0.208±0.001	0.386±0.002
Water	0.210±0.001	0.389±0.002

As shown in this table, the relative difference of the absorbed dose delivered to brain with polyacrylamide gel and water is 0.00% and 0.96% in the 6MV radiation field, respectively. Furthermore, this difference in the radiation field of 18MV is 0.26% and 0.52% for polyacrylamide gel and water, respectively.

4 Conclusion

In head and neck phantoms, usually water is used as brain equivalent material. Although this material is a suitable substitute for brain, it cannot be used as a dosimeter. So, in order to determine the

2020 JINST 15 P03016

absorbed dose delivered to it different dosimeters such as ionization chamber, thermoluminescence dosimeters, gaff chromic films etc. have to be used. The type of these dosimeters differs from water, also these dosimeters cannot be used for determination of three dimensional dose distribution. These issues are the major concerns in validation of the algorithms used for treatment planning systems. In this study, a feasible study of using polyacrylamide gel as brain equivalent material has been performed. The results reveals that the values of the mass energy absorption coefficient, mass stopping power, effective atomic number, mass attenuation coefficient and delivered absorbed dose of polyacrylamide gel and brain are close to each other. It means that similar to water, the polyacrylamide gel can be also used as brain equivalent material in designing and construction of head and neck phantoms. Polyacrylamide is known as a reliable dosimeter of X and Gamma rays. Also, this material can be used for determination of the three dimensional dose distribution. Consequently, in designing and construction of head and neck phantoms, polyacrylamide gel can be used as brain equivalent martial applicable for determination of the three dimensional dose distribution. Moreover, the price of polyacrylamide gel is low and it can be formed in different sizes and shapes.

References

[1] Y. Cao et al., *Superficial dose evaluation of four dose calculation algorithms*, *Radiat. Phys. Chem.* **137** (2017) 23.

[2] A. Fogliata et al., *Dosimetric evaluation of Acuros XB Advanced Dose Calculation algorithm in heterogeneous media*, *Radiat. Oncol.* **6** (2011) 82.

[3] Y.L. Kim et al., *Dose distribution evaluation of various dose calculation algorithms in inhomogeneous media*, *Int. J. Radiat. Res.* **14** (2016) 269.

[4] G. Kragl, D. Albrich and D. Georg, *Radiation therapy with unflattened photon beams: dosimetric accuracy of advanced dose calculation algorithms*, *Radiotherapy Oncology* **100** (2011) 417.

[5] J. Ojala, *The accuracy of the Acuros XB algorithm in external beam radiotherapy — a comprehensive review*, *Int. J. Canc. Ther. Oncol.* **2** (2014) 020417.

[6] P.S. Kroon, S. Hol and M. Essers, *Dosimetric accuracy and clinical quality of Acuros XB and AAA dose calculation algorithm for stereotactic and conventional lung volumetric modulated arc therapy plans*, *Radiat. Oncol.* **8** (2013) 149.

[7] C.M. Ma et al., *Monte Carlo verification of IMRT dose distributions from a commercial treatment planning optimization system*, *Phys. Med. Biol.* **45** (2000) 2483.

[8] P.C.Y. Yeh et al., *Monte Carlo evaluation of Acuros XB dose calculation Algorithm for intensity modulated radiation therapy of nasopharyngeal carcinoma*, *Radiat. Phys. Chem.* **140** (2017) 419.

[9] M. Bueno et al., *Experimental verification of Acuros XB in the presence of lung-equivalent heterogeneities*, *Radiat. Meas.* **106** (2017) 357.

[10] S.S. Al-Ahbabi, D. Bradley and A. Nisbet, *Tomotherapy evaluation for head and neck cases using two types of phantoms*, *Radiat. Phys. Chem.* **95** (2014) 323.

[11] L. Wang, E. Yorke and C.-S. Chui, *Monte Carlo evaluation of tissue inhomogeneity effects in the treatment of the head and neck*, *Int. J. Radiat. Oncol. Biol. Phys.* **50** (2001) 1339.

2020 JINST 15 P03016

[12] K. Eng, S. Kandaiya and N. Yahaya, *Radiotherapy dose verification on a customised head and neck perspex phantom*, *J. Phys. Conf. Ser.* **851** (2017) 012020.

[13] K.M. Radaideh et al., *Development and evaluation of a Perspex anthropomorphic head and neck phantom for three dimensional conformal radiation therapy (3D-CRT)*, *J. Radiother. Pract.* **12** (2013) 272.

[14] J.W. Brand, R.K. Kuba and T.C. Braunreiter, *An improved head-and-neck phantom for radiation dosimetry*, *Oral Surg. Oral Med. Oral Pathol.* **67** (1989) 338.

[15] G.J. Webster et al., *Design and implementation of a head-and-neck phantom for system audit and verification of intensity-modulated radiation therapy*, *J. Appl. Clin. Med. Phys.* **9** (2008) 46.

[16] A.H. Aitkenhead, C.G. Rowbottom and R.I. Mackay, *Marvin: an anatomical phantom for dosimetric evaluation of complex radiotherapy of the head and neck*, *Phys. Med. Biol.* **58** (2013) 6915.

[17] H. Kitamori et al., *Evaluation of mouthpiece fixation devices for head and neck radiotherapy patients fabricated in PolyJet photopolymer by a 3D printer*, *Phys. Med.* **58** (2019) 90.

[18] C. Ferreira et al., *Evaluation of tissue-equivalent materials to be used as human brain tissue substitute in dosimetry for diagnostic radiology*, *Nucl. Instrum. Meth.* **B 268** (2010) 2515.

[19] P. von Voigts-Rhetz et al., *Perturbation correction for alanine dosimeters in different phantom materials in high-energy photon beams*, *Phys. Med. Biol.* **61** (2016) N70.

[20] A. Boni, *A polyacrylamide gamma dosimeter*, *Radiat. Res.* **14** (1961) 374.

[21] P. Mann, A. Schwahofer and C.P. Karger, *Absolute dosimetry with polymer gels — A TLD reference system*, *Phys. Med. Biol.* **64** (2019) 045010.

[22] A. Jirasek et al., *Investigation of tetrakis hydroxymethyl phosphonium chloride as an antioxidant for use in x-ray computed tomography polyacrylamide gel dosimetry*, *Phys. Med. Biol.* **51** (2006) 1891.

[23] H. Khosravi, F. Rahmani and B. Hashemi, *Gel dosimetry: The effect of gold nanoparticles on the dose enhancement in the external radiation therapy*, *Nanomed. Res. J.* **1** (2016) 31.

[24] S.-i. Hayashi et al., *Influence of magnesium chloride on the dose-response of polyacrylamide-type gel dosimeters*, *Radiol. Phys. Technol.* **11** (2018) 375.

[25] M. Maryanski et al., *Magnetic resonance imaging of radiation dose distributions using a polymer-gel dosimeter*, *Phys. Med. Biol.* **39** (1994) 1437.

[26] J. Gore et al., *Radiation dose distributions in three dimensions from tomographic optical density scanning of polymer gels: I. Development of an optical scanner*, *Phys. Med. Biol.* **41** (1996) 2695.

[27] M. Hilts, *X-ray computed tomography imaging of polymer gel dosimeters*, *J. Phys. Conf. Ser.* **56** (2006) 95.

[28] C. Baldock et al., *Fourier transform Raman spectroscopy of polyacrylamide gels (PAGs) for radiation dosimetry*, *Phys. Med. Biol.* **43** (1998) 3617.

[29] M.L. Mather, A.K. Whittaker and C. Baldock, *Ultrasound evaluation of polymer gel dosimeters*, *Phys. Med. Biol.* **47** (2002) 1449.

[30] D. White et al., *ICRU Report 44: Tissue Substitutes in Radiation Dosimetry and Measurement*, *J. ICRU* **os23** (1989).

[31] J. Hubbell and S. Seltzer, *Tables of X-ray mass attenuation coefficients and mass energy-absorption coefficients (version 1.4)*, National Institute of Standards and Technology, Gaithersburg, MD (2004).

2020 JINST 15 P03016

[32] C. Suplee, *Stopping-Power & Range Tables for Electrons, Protons, and Helium Ions*, NIST Standard Reference Database 124 (2009) [DOI].

[33] M. Taylor et al., *Robust calculation of effective atomic numbers: The Auto-Zeff software*, *Med. Phys.* **39** (2012) 1769.

[34] J.F. Briesmeister, *MCNP4C Monte Carlo N-Particle Transport Code System*, MCNP-4C, Monte Carlo N-Particle Transport Code System (2000).

[35] W.S. Snyder et al., *Estimates of absorbed fractions for monoenergetic photon sources uniformly distributed in various organs of a heterogeneous phantom*, Oak Ridge National Lab., Tenn (1969).

[36] D. Sheikh-Bagheri and D.W.O. Rogers, *Monte Carlo calculation of nine megavoltage photon beam spectra using the BEAM code*, *Med. Phys.* **29** (2002) 391.

[37] M. Lybanon, *A better least-squares method when both variables have uncertainties*, DTIC Document (1984).

2020 JINST 15 P03016